Catalytic and Bulk Solvent Effects on Proton Transfer: Formamide As a Case Study

CARLO ADAMO,* MAURIZIO COSSI, VINCENZO BARONE

Dipartimento di Chimica, Università Federico II, via Mezzocannone 4, I-80134 Napoli, Italy

Received 7 May 1997; accepted 17 July 1997

ABSTRACT: Structural, thermodynamic, and kinetic aspects of the tautomerization of formamide through direct and solvent-assisted proton transfer have been investigated. Both specific and bulk effects of the solvent play a role in determining the overall result so that only a mixed discrete-continuum model is sufficiently reliable. Structural modifications induced by the solvent are significant, but have only a slight effect on thermodynamic and kinetic quantities. The same remarks apply to the vibrational shifts induced by the solvent.
 J Comput Chem **18**: 1993–2000, 1997

Keywords: proton transfer; solvent effects; formamide; adiabatic connection methods

Introduction

Proton transfer between different molecules or between different moieties of the same molecule plays a crucial role in a number of processes ranging from acid/base neutralization to enzymatic reactions and to tautomeric interconversions in DNA bases.[1, 2] As a consequence, the availability of a general quantum mechanical protocol for computing the static and dynamic properties of this process would be very valuable. At the same time, such a computational procedure should be amenable to interpretation in terms of chemical concepts like charge transfer, resonance effects, and so on. This target is quite ambitious, especially concerning biomolecules, due to the large dimensions of even the smallest realistic models coupled to the significance of many body effects in noncovalent interactions. Matters are further complicated by the role of quantum effects like tunneling, or corner cutting[3] in the dynamics of proton transfer (PT). Moreover, environmental effects are not negligible, with the solvent often playing the role of a true catalyst (i.e., the reaction mechanism *in vacuo* is modified through the direct involvment of

* *Permanent address:* Dipartimento di Chimica, Università della Basilicata, via N. Sauro 85, I-85 100 Potenza, Italy

Correspondence to: V. Barone; e-mail: enzo@chemna.dichi.unina.it

CCC 0192-8651 / 97 / 161993-08

specific solvent molecules) modulated by the selective stabilization of more polar species by the reaction field of the bulk.[4]

We have been concerned in recent years[4–7] with the description of the most significant aspects of PT in ground and excited electronic states. Here, we concentrate our attention on the role of the solvent with special reference to the interplay of direct and indirect effects. In the first category we include electrostatic solute–solute interactions together with polarization effects.[8] Indirect effects are, instead, related to structural modifications of the solute induced by the solvent, which, in turn, can affect the energetics and dynamics of PT.[4,9]

To analyze both these aspects we need a reliable and effective solvent model allowing geometry optimization by analytical derivatives. Polarizable continuum models have become, in recent years, reliable enough to compete with numerical simulations especially when combined discrete-continuum approaches are employed.[8,10,11] Furthermore, several implementations of analytic energy derivatives[12–19] have been also reported. In this study we will apply our version of the polarizable continuum model (PCM)[19–21] for a number of systems in which the solute and the few solvent molecules directly entering the reaction mechanism are treated at the microscopic level, whereas the bulk of the solvent is represented by a polarizable dielectric. We will consider, in particular, the direct and solvent-assisted *keto-enol* tautomerization of the simplest amide, formamide. Together with its intrinsic interest, the formamide moiety represents the simplest building block of DNA bases without the perturbing effects of further functional groups and of aromaticity. As such, it has been considered by several investigators[22–27] a significant benchmark for new computational approaches.

From another point of view, composite techniques, like the so-called G2(MP2) method,[28] have proven to be very cost effective in the computation of accurate energetic quantities. In these methods geometry optimization and computation of non–potential energy effects (e.g., zero-point energy, ZPE, etc.) are performed at a lower level and better estimates of energetic quantities are obtained through single-point computations by more refined procedures.

Because the replacement of HF by DF methods in the first step of such procedures seems very effective for *in vacuo* studies,[29,30] here we propose the extension of the same philosophy to solution studies adding to standard G2 results geometric and energetic solvent shifts computed by a DF approach.

Computational Details

All the DF computations are based on the Kohn–Sham (KS) approach to the DF theory[31] as implemented in the Gaussian 94 (G94) package.[32] On the basis of previous experience,[4,5,7] we have selected the so-called B3LYP hybrid functional, which combines Hartree–Fock (HF) and Becke exchange[33] terms with the Lee–Yang–Parr correlation functional,[34] in the same ratios as those optimized by Becke for a similar (although nonidentical) functional.[35] Most of the computations have been performed by the popular 6-31G(d, p) basis set.[36] Basis set saturation effects have been investigated employing a triple-ζ description of the valence space with double sets of polarization functions (hereafter referred to as the TZ2P basis set), already tested for DF computations.[37]

Post-HF computations have been performed by the same package using both second-order many-body perturbation theory (MP2)[38] and the coupled clusters approach, including single, double, and a perturbative estimate of triple excitations [CCSD(T)].[39] In these computations we have used also the 6-311G(d, p) and 6-311 + G(3df, 2p) basis sets.[40]

In particular, our best estimates of reaction (ΔE) and activation ($\Delta E^{\#}$) energies (broadly referred to as G2M values) are obtained adding to CCSD(T)/6-311G(d, p) energies obtained at B3LYP/6-31G(d, p) geometries the energy differences between MP2 computations performed at the same geometries with the small [6-311G(d, p)] or large [6-311 + G(3df, 2p)] basis set. Because empirical higher level correction terms (as required in general for a G2-type procedure) effectively cancel out in the computation of activation and reaction energies for tautomerizations, this procedure corresponds to that recently proposed in ref. 29 to improve the standard G2(MP2) approach.

Solvent shifts and non–potential energy effects computed at the B3LYP/6-31G(d, p) level are also included. In particular, bulk solvent effects are taken into account by PCM employing a cavity formed by interlocking spheres centered on the different atoms[41,42] with radii proportional to van der Walls values (1.2, 1.5, 1.5, and 1.4 Å for H, C,

N, and O, respectively, and 1.0 Å when H is bonded to electronegative atoms[20]). The free energy of a molecule in solution is written as a sum of contributions:

$$G = G_{el} + G_{cav} + G_{disp} + G_{rep} \qquad (1)$$

$G_{cav}, G_{disp}, G_{rep}$ collectively referred to as nonelectrostatic terms, describe the energy needed to build the cavity and the solute solvent dispersion–repulsion interactions, respectively. These terms, together with their gradients, are calculated by classical approaches, described elsewhere.[42–44] On the other hand, the electrostatic contribution modifies the quantum-mechanical Hamiltonian of the solute, thus affecting both the total energy and the electron density. The expression for this term and its derivatives have been given elsewhere,[17] as is also the case for our recent implementation in the Gaussian series of programs.[19,20]

Second derivatives have been computed in some cases using central finite differences of analytical gradients. This has allowed an estimation of solvent-induced shifts of harmonic vibrational frequencies. Furthermore, non–potential energy effects on thermodynamic and kinetic parameters have also been obtained by well-known statistic thermodynamical equations based on the rigid rotor-harmonic oscillator approximation.

Results and Discussion

Proton transfer between the —NH_2 and $>$CO moieties can be direct or assisted by specific water molecules (Fig. 1). In the latter case, the rate for the PT reaction depends strongly on the lifetime of the complex involving the amphiprotic molecules. Although either one or two water molecules could be involved in the mechanism on energetic grounds, numerical simulations[45] indicate that only one molecule is bridge bonded between the two sites of formamide for a sufficient time. As a consequence we will consider only this situation in what follows. Although the direct process is unlikely to occur in water, it will be analyzed in detail to separate catalytic and bulk solvent effects.

The optimized bond lengths and valence angles of formamide (F), formamidinic acid (FA), and of the corresponding saddle point (SP) are reported in Table I together with the experimental structure of formamide.[46] A detailed comparison with previous MP2 results[24] confirms that good geometrical parameters are provided by the B3LYP approach,

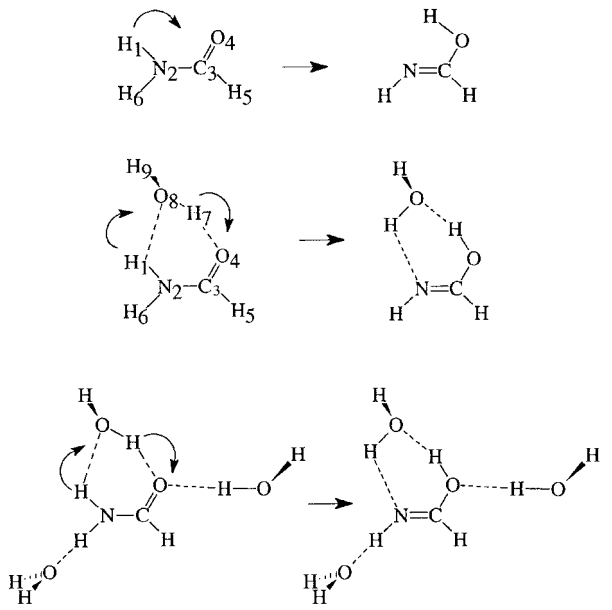

FIGURE 1. Schematic drawings of direct and assisted (either by one or two water molecules) proton transfer leading from formamide to formamidinic acid. The atom numbering is also indicated.

at least for structures corresponding to energy minima.[29,30] This consideration is supported also by the good agreement between computed and experimental structural parameters for F. The situation could be, in principle, more involved for the SP structure, because several studies have shown that DF approaches suffer from severe limitations in determining the structures of SP characterizing PT reactions (see, e.g., ref. 5). Anyway, our previous experience shows that the B3LYP approach also gives, in such delicate situations, geometrical parameters remarkably close to those obtained by post-HF approaches.[4,7] Furthermore, the results obtained with the extended TZ2P basis set show that geometrical parameters are essentially converged with respect to basis set extension. This confirms that, at least concerning geometrical features, the B3LYP method is not particularly sensitive to the choice of basis set. Also, the harmonic frequencies and IR intensities computed at the B3LYP/6-31G(d, p) level are in good agreement with MP2/6-31G(d, p) results and with the experimental data recorded in argon matrix.[46]

The formation of the adduct with one water molecule induces some significant variations in the internal geometrical parameters of F, essentially related to the stabilization of resonance structures involving a formal charge separation [here $H_2N^+=C(H)—O^-$ vs. $H_2N—C(H)=O$]. In par-

TABLE I.
Bond Lengths (Angstroms) and Angles (Degrees) of Formamide (F), Formamidinic Acid (FA), and the Corresponding Saddle Point (SP), Optimized at the B3LYP Level in Both the Gas Phase and in Aqueous Solution.

	Gas phase							Aqueous solution		
	F			SP		FA		F	SP	FA
	6-31G(d, p)	TZ2P	Exp.[a]	6-31G(d, p)	TZ2P	6-31G(d, p)	TZ2P	6-31G(d, p)	6-31G(d, p)	6-31G(d, p)
N_2—H_1	1.007	1.003	1.002	1.335	1.337	2.306	2.298	1.011	1.344	2.295
N_2—H_6	1.009	1.005	1.002	1.014	1.009	1.019	1.014	1.009	1.015	1.019
N_2—C_3	1.361	1.359	1.360	1.303	1.297	1.267	1.261	1.341	1.296	1.267
C_3—O_4	1.216	1.211	1.219	1.285	1.281	1.347	1.348	1.233	1.299	1.347
C_3—H_5	1.109	1.101	1.098	1.091	1.085	1.094	1.088	1.104	1.088	1.095
O_4—H_1	2.550	2.544	2.547	1.329	1.333	0.973	0.968	2.514	1.316	0.973
N_2—O_4	2.286	2.277	2.283	2.095	2.101	2.287	2.283	2.288	2.102	2.288
H_1—N_2—C_3	121.7	121.1	121.4	73.0	72.9	54.9	53.7	120.5	73.3	53.8
H_1—O_4—C_3	52.5	51.3	51.5	73.1	73.3	110.0	106.9	54.0	74.1	106.1
H_6—N_2—C_3	118.9	119.5	118.8	125.5	125.5	110.9	111.6	120.5	124.5	110.8
O_4—C_3—N_2	124.9	124.7	124.5	108.6	108.6	122.0	122.1	125.3	108.2	122.1
H_5—C_3—N_2	112.0	112.5	112.7	128.5	128.6	128.0	127.5	112.6	128.9	128.0

[a] Ref. 46.

ticular, the CO bond length increases by 0.014 Å and the CN bond length decreases by 0.013 Å. Similar variations, but in the opposite direction, are found for the *enol* tautomer, which forms stronger H-bonds.[48] To allow a further check of the soft intermolecular geometrical parameters obtained by the B3LYP approach we have performed complete geometry optimizations of F, SP, and FA adducts at the MP2/6-31G(d, p) level. The results shown in Table II indicate that, as already found for similar water–adduct complexes,[4] the B3LYP and MP2 approaches give very similar intermolecular parameters.

The geometries optimized in aqueous solution are also reported in Tables I and II. The role of the solvent reaction field in stabilizing the dipolar resonance structure of F is quite apparent. So, in the bare formamide, a lengthening of the CO bond (+0.017 Å) and a shortening of the CN bond (−0.020 Å) are found. These results are consistent with a decreasing of the double bond character of the CO bond and an increasing of the double bond character of the CN bond. On the contrary the geometry of the less polar *enol* form is not significantly affected by the solvent field, whereas an intermediate behavior is found for the SP. Although less evident, these effects are still present in the adduct with one water molecule, thus suggesting that bulk solvent further increases the effects due to specific interactions. All these trends are similar to those obtained in ref. 28 by a related solvent model employing a one-center multipolar expansion of the solute electric field.

The geometrical rearrangments induced by the solvent are reflected in the infrared (IR) spectra, especially that of F (See Fig. 2). Although no mode mixing is observed in going from the gas phase to aqueous solution, a large shift of the carbonyl stretching is induced in F by the solvent (+90 cm^{-1}). Other significant solvent shifts are calculated for the CH stretching (+63 cm^{-1}) and for the out-of-plane bending of the amine moiety (+206 cm^{-1}). The solvent effect on the CO stretching is in agreement with experimental observations on several carbonyl compounds[24] and all the computed shifts are consistent with the stabilization by the solvent of the resonance structure involving a formal charge separation. Accordingly, the less polar *enol* tautomer experiences smaller vibrational shifts in going from the gas phase to aqueous solution. As expected, the IR intensities of the strongest bands are larger in aqueous solution than *in vacuo*. Once again, the adduct with one water molecule shows the same general trends, which are, however, significantly smoothed by the separate consideration of specific interactions of F with a single water molecule.

It must be emphasized that interactions with a specific solvent molecule modify the very mechanism of PT (from direct to assisted, see Fig. 1), whereas bulk solvent effects only induce a further fine tuning. This is well evidenced by the quite

TABLE II.
Optimized Bond Lengths (Angstroms) and Angles (Degrees) of Stationary Points Characterizing the Tautomerization of Formamide Complexes with One Water Molecule, in both the Gas Phase and in Aqueous Solutions.

	Gas phase									Aqueous solution[a]		
	F			SP			FA			F	SP	FA
	A	B	C	A	B	C	A	B	C	A	B	C
N_2—H_1	1.022	1.014	1.015	1.318	1.302	1.311	2.343	2.348	2.342	1.017	1.335	1.930
N_2—H_6	1.007	1.002	1.003	1.012	1.007	1.009	1.017	1.012	1.015	1.010	1.011	1.017
N_2—C_3	1.348	1.346	1.349	1.308	1.303	1.309	1.280	1.272	1.284	1.333	1.303	1.273
C_3—O_4	1.230	1.223	1.236	1.284	1.283	1.289	1.328	1.330	1.334	1.243	1.295	1.338
C_3—H_5	1.105	1.099	1.099	1.097	1.090	1.091	1.095	1.088	1.088	1.100	1.094	1.092
O_4—H_7	1.899	1.895	1.941	1.220	1.206	1.223	0.999	0.989	0.990	1.852	1.273	0.996
O_4—O_8	2.800	2.793	2.833	2.397	2.399	2.387	2.611	2.627	2.724	2.794	2.401	2.708
O_8—H_9	0.966	0.959	0.962	0.967	0.961	0.966	0.966	0.960	0.963	0.967	0.970	0.969
O_8—H_1	1.975	2.060	2.017	1.192	1.209	1.184	0.988	0.981	0.979	2.075	1.175	0.986
O_8—N_2	2.840	2.842	2.875	2.415	2.416	2.399	2.739	2.760	2.781	2.917	2.411	2.789
H_1—N_2—C_3	11706	118.9	117.9	105.3	105.7	105.1	55.6	54.9	55.4	118.5	105.9	104.4
H_6—N_2—C_3	121.0	120.5	120.6	116.6	116.9	116.0	111.4	111.7	111.4	120.8	116.1	109.2
O_4—C_3—N_2	124.9	124.9	124.9	122.0	121.7	122.0	123.5	123.4	123.3	124.3	121.6	123.4
H_5—C_3—N_2	113.8	113.7	113.6	121.3	121.4	121.3	125.2	125.2	125.5	114.4	122.3	125.1
H_7—O_4—C_3	105.6	107.2	105.5	103.2	103.5	102.4	111.3	108.6	111.4	105.2	102.2	107.9
H_9—O_8—H_7	104.3	106.3	104.0	109.5	110.9	109.0	104.9	106.4	104.5	107.2	107.1	103.8
H_9—O_8—H_7—O_4	112.0	113.6	104.3	108.2	109.9	111.4	109.8	107.8	105.1	101.0	106.4	104.3

[a] A: B3LYP / 6-31G(d, p); B: B3LYP / TZ2P; C: MP2 / 6-31G(d, p).

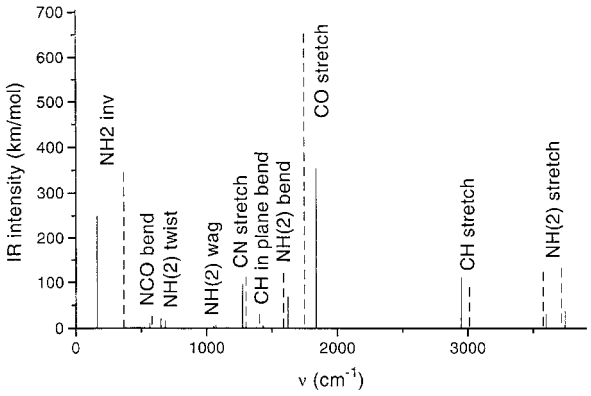

FIGURE 2. Harmonic frequencies and IR intensities computed for formamide at the B3LYP / 6-31G(d, p) level *in vacuo* (solid lines) and in aqueous solution (broken lines).

similar structure and transition vector of the SP governing assisted PT *in vacuo* and in aqueous solution (see Fig. 3).

The thermochemistry of direct and water-assisted tautomerization of formamide is summarized in Table III. Let us start the discussion from the gas-phase results. The B3LYP method predicts that F is more stable than FA by 12.6 kcal/mol, close to the MP2/6-31G(d, p) estimate (12.7 kcal/mol).[24] Extension of the basis set slightly reduces the B3LYP result (to 12.0 kcal/mol), which is now very close to the QCISD value obtained by the 6-31 + G(d, p) basis set at MP2/6-31G(d, p) geometries (11.7 kcal/mol),[24] and well within the range of experimental estimate (11 ± 4 kcal/mol). The further inclusion of ZPE effects does not alter these results. The activation energy governing direct PT is very high (46.2 kcal/mol) at the B3LYP/6-31G(d, p) level, this value being confirmed by a previous MP2 computation (45.2 kcal/mol).[9] As already found for other PT reactions,[4,5] in DF methods, extension of the basis set generally increases the activation (+1.3 kcal/mol), and so our best estimate 44.4 kcal/mol, including ZPE corrections.

The specific interaction with a water molecule significantly stabilizes the *enol* tautomer with respect to the *keto* one, for its ability to form stronger hydrogen bonds.[5,48] As a consequence, a reduction of the endothermicity by (2.5 kcal/mol) is found at the B3LYP/6-31G(d, p) level. A much more dramatic effect is observed on the activation energy, which is reduced to less than half the original value (19.4 vs. 46.2 kcal/mol) in the adduct with one water molecule. This is due, of course, to the catalytic role played by a specific solvent molecule,

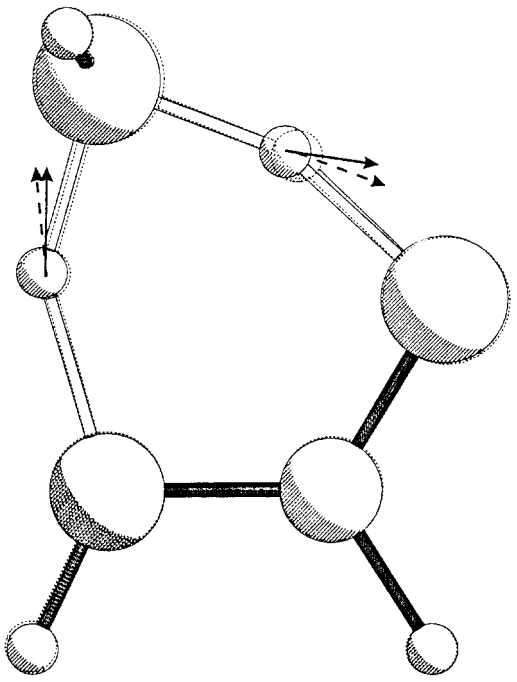

FIGURE 3. Transition structures and transition vectors governing assisted proton transfer *in vacuo* (solid lines) and in aqueous solution (broken lines).

which modifies the reaction mechanism. In this case, basis set extension and inclusion of ZPE corrections lead to a final estimate of 19.1 kcal/mol.

The thermodynamics and kinetics of assisted PT have been next investigated by the modified G2 procedure discussed in the Computational Details section. The results of Table IV show that the effects of basis set extension and of more complete inclusion of correlation are quite small in the computation of the energy barrier, so that the MP2/6-31G(d, p) value (22.4 kcal/mol) is close to the G2 one (23.3 kcal/mol). Also, the B3LYP/TZ2P result (21.4 kcal/mol) is satisfactory, but in this case the smaller 6-31G(d, p) basis set is less adequate ($\Delta E^{\#}$ = 19.4 kcal/mol). The same general remarks apply to the reaction energy, but in this case the effect of basis set extension is small by all the methods employed, whereas the difference between CCSD(T) and MP2 computations is not completely negligible. As expected, the B3LYP value is satisfactory for this quantity without further corrections.

From another point of view, MP2 results are nearly identical using B3LYP or MP2 geometries, whereas significantly different values (ΔE = 9.2 kcal/mol, $\Delta E^{\#}$ = 18.9 kcal/mol) are obtained using HF/6-31G(d, p) geometries.[9] This confirms the impact of geometry optimization using correlated methods[29,30,49] and further strengthens the merits of the B3LYP approach, which is able to recover these effects with essentially the same computational requirements as the HF method.

We next estimated the effect of the bulk solvent reaction field on the endothermicity and on the activation energy of the *keto–enol* tautomerization. In an attempt to reach a sharp separation between direct and indirect contributions, we first carried out some computations in solution using gas-phase geometries. Our results show that solvent effects are particularly significant for the bare molecule, where the endothermicity is increased by 3.3 kcal/mol and the activiation energy by 4.0 kcal/mol, with respect to the corresponding gas-phase values. Although comparatively smaller, bulk solvent effects are not negligible for assisted PT, thus increasing the endothermicity computed for the bare adduct by 2.7 kcal/mol and the activation energy by 2.3 kcal/mol. Geometry reoptimization in the presence of bulk solvent increases the values computed using geometries optimized *in vacuo* by 10–15%. In particular, both the endothermicity and activation energy of assisted PT increase by about 0.5 kcal/mol. This is due to the

TABLE III.
Main Energy Contributions (in Kilocalories per Mole) to Endothermicities (ΔE) and Activation Energies ($\Delta E^{\#}$) for *Keto/Enol* Tautomerization of Formamide Obtained by B3LYP Approach.

	Intrinsic[a]	ΔZPE[a]	Δ (Basis set extension)[b]	Δ (Solvent)[a,c]
ΔE_{dir}	12.6	0.1	−0.6	3.6(3.3)
$\Delta E^{\#}_{dir}$	46.2	−3.1	1.3	4.4(4.0)
ΔE_{asst}	10.1	0.3	0.1	2.9(2.3)
$\Delta E^{\#}_{asst}$	19.4	−3.3	2.0	2.0(1.4)

[a] 6-31G(d, p); [b] TZ2P basis set; [c] in parantheses are values computed using geometries optimized *in vacuo*.

TABLE IV.
Post-HF Computations of Thermodynamic and Kinetic Parameters for Assisted Proton Transfer. Only Valence Electrons Included in Correlation Treatments (See Text).

	MP2 6-31G(d, p)[a]	MP2 6-31G(d, p)[b]	MP2 6-311G(d, p)[a]	MP2 6-311 + G(3df, 2p)[a]	CCSD(T) 6-311G(d, p)[a]	G2M[a]	B3LYP TZ2P[a]
$E(F[H_2O])$[c]	−245.66106	−245.66137	−245.77708	−245.93857	−245.82266		
ΔE^{d}_{asst}	10.5	10.5	9.3	10.3	8.5	9.6	10.0
$\Delta E^{\#d}_{asst}$	22.4	22.5	22.1	22.4	23.3	23.3	21.4

[a] At B3LYP / 6-31G(d, p) geometries; [b] at MP2 / 6-31G(d, p) geometries; [c] in a.u; [d] in kilocalories per mole.

fact that only the geometry of F is significantly modified by bulk solvent with a consequent selective stabilization of this species. Once again, this effect can be traced back to an increased weight of the resonance structure involving a formal charge separation.

Conclusion

In this study, we have reported on a comprehensive study of the kinetics and thermodynamics of direct and water-assisted proton transfer in formamide. Our results show that both equilibrium and nonequilibrium solvent effects modify the thermodynamics of the reaction, but for different reasons. Bulk solvent stabilizes formamide due to its higher dipole moment, whereas the specific interaction with a water molecule provides the opposite trend due to the ability of formamidinic acid to form stronger hydrogen bonds. Note, however, that this last remark is at least partly misleading because coordination of further water molecules at the carbonyl oxygen atom is favored for formamide.[48] Furthermore, a discrete model including only the first solvation shell is not sufficient because the bulk effect of water is different for the two tautomers. The same remarks apply to the kinetics of the reaction, but solvent effects are lower due to the similar electronic structures for formamide and SP.

From another point of view, the B3LYP approach, although somewhat underestimating PT barriers for flexible systems, provides very good structural and thermodynamical data. Geometry optimization can be effectively performed in solution and leads to non-negligible modifications with respect to the structures obtained for isolated molecules. On the other hand, the effect of geometry optimization in solution on the energetic quantities (i.e., endothermicity and activation barrier) is less pronounced. The solvent effect is also significant in regard to vibrational frequencies and IR intensities; however, in this case, the kinetics and thermodynamics of tautomerization are not affected, because the effects of vibrational shifts are smeared out in the computation of non−potential energy effects. From a more general point of view, the development of effective DF approaches, including some HF exchange (here B3LYP) and refined continuum solvent models (here PCM), is paving the route for complete quantum mechanical studies of PT in realistic models of biomolecules.

References

1. G. W. Robinson, P. J. Thistlethwaite, and J. Lee, *J. Phys. Chem.*, **90**, 4224 (1986).
2. G. A. Jeffrey and W. Saenger, *Hydrogen Bonding in Biological Structures*, Springer, Berlin, 1991.
3. V. A. Benderskii, D. E. Makarov, and C. A. Wight, *Adv. Chem. Phys.*, **88**, 1 (1994).
4. V. Barone and C. Adamo, *J. Phys. Chem.*, **99**, 15062 (1995).
5. V. Barone, L. Orlandini, and C. Adamo, *Chem. Phys. Lett.*, **231**, 295 (1994).
6. V. Barone and C. Adamo, *Chem. Phys. Lett.*, **241**, 1 (1995).
7. V. Barone and C. Adamo, *J. Chem. Phys.*, **105**, 11007 (1996).
8. J. Tomasi and M. Persico, *Chem. Rev.*, **94**, 2027 (1994), and references therein.
9. X. C. Wang, J. Nichols, M. Feyereisen, M. Gutowski, J. Boatz, A. D. J. H. Haymet, and J. Simons, *J. Phys. Chem.*, **95**, 10419 (1991).
10. J. L. Rivail, D. Rinaldi, and M. F. Ruiz-López, *Liquid State Quantum Chemistry in Computational Chemistry: Review of Current Trends*, J. Lesczynski, Ed., World Scientific, Singapore, 1995.
11. C. J. Cramer, D. J. Truhlar, In *Reviews in Computational Chemistry, Vol. 6.*, K. B. Lipkowitz and B. Boyd, Eds., VCH, New York, 1995.
12. I. Tuñon, M. F. Ruiz-López, D. Rinaldi, and J. Bertran, *J. Comput. Chem.*, **17**, 148 (1996).
13. T. N. Truong and E. V. Stefanovich, *J. Chem. Phys.*, **103**, 3709 (1995) and **105**, 2961 (1996).

14. J. Andzelm, C. Kölmel, and A. Klamt, *J. Chem. Phys.*, **103**, 9312 (1995).
15. C. M. Cortis, J. M. Langlois, M. D. Beachy, and R. A. Friesner, *J. Chem. Phys.*, **105**, 5472 (1996).
16. V. Dillet, D. Rinaldi, J. Bertran, and J. L. Rivail, *J. Chem. Phys.*, **104**, 9437 (1996).
17. R. Cammi and J. Tomasi, *J. Chem. Phys.*, **100**, 7495 (1994).
18. K. Baldridge and A. Klamt, *J. Chem. Phys.*, **106**, 6622 (1997).
19. V. Barone, M. Cossi, and J. Tomasi, manuscript submitted.
20. M. Cossi, V. Barone, R. Cammi, and J. Tomasi, *Chem. Phys. Lett.*, **255**, 327 (1996); N. Rega, M. Cossi, and V. Barone, *J. Chem. Phys.*, **105**, 11060 (1996).
21. V. Barone, M. Cossi, and J. Tomasi, *J. Chem. Phys.*, in press.
22. M. J. Frisch, G. W. Trucks, H. B. Schlegel, P. M. W. Gill, B. G. Johnson, M. A. Robb, J. R. Cheeseman, T. A. Keith, G. A. Petersson, J. A. Montgomery, K. Raghavachari, M. A. Al-Laham. V. G. Zakrewski, J. V. Ortiz, J. B. Foresman, J. Cioslowski, B. B. Stefanov, A. Nanayakkara, M. Challacombe, C. Y. Peng, P. Y. Ayala, W. Chen, M. W. Wong, J. L. Andres, E. S. Replogle, R. Gomperts, R. L. Martin, D. J. Fox, J. S. Binkley, D. J. DeFrees, J. Baker, J. P. Stewart, M. Head-Gordon, C. Gonzalez, and J. A. Pople, *Gaussian*-94 (Revision D.4). Gaussian Inc., Pittsburgh, PA, 1996.
23. V. Barone and M. Cossi, submitted for publication.
24. M. K. Wong, K. B. Wiberg, and M. J. Frisch, *J. Am. Chem. Soc.*, **114**, 1645 (1992).
25. F. Sim, A. St. Amant, I. Papai, and D. R. Salahub, *J. Am. Chem. Soc.*, **114**, 4391 (1992).
26. J. C. Contador, M. L. Sanchez, M. A. Aguillar, and F. J. Olivares del Valle, *J. Chem. Phys.*, **104**, 5539 (1996).
27. J. S. Craw, J. M. Guest, M. D. Copper, N. A. Burton, and I. H. Hillier, *J. Phys. Chem.*, **100**, 6304 (1996).
28. S. Antonczak, M. F. Ruiz-López, and J. L. Rivail, *J. Am. Chem. Soc.*, **116**, 3912 (1994).
29. L. A. Curtiss, K. Raghavachari, and J. A. Pople, *J. Chem. Phys.*, **98**, 1293 (1993).
30. C. W. Bauschlicher and H. Partridge, *J. Chem. Phys.*, **103**, 1788 (1995).
31. A. M. Mabel, K. Morokuma, and M. C. Liu, *J. Chem. Phys.*, **103**, 7415 (1995).
32. R. G. Parr and W. Yang, *Density Functional Theory of Atoms and Molecules*, Oxford University Press, Oxford, UK, 1989.
33. A. D. Becke, *Phys. Rev. B*, **38**, 3098 (1988).
34. C. Lee, W. Yang, and R. G. Parr, *Phys. Rev. B*, **37**, 785 (1988).
35. A. Becke, *J. Chem. Phys.*, **98**, 5648 (1993).
36. W. J. Hehre, R. Ditchfield, and J. A. Pople, *J. Chem. Phys.*, **56**, 2257 (1972).
37. N. Oliphant and R. J. Bartlett, *J. Chem. Phys.*, **100**, 6550 (1994).
38. J. A. Pople, J. S. Binkley, and R. Seeger, *Int. J. Quantum Chem. Quantum Chem. Symp.*, **10**, 1 (1976).
39. J. A. Pople, M. Head-Gordon, and K. Raghavachari, *J. Chem. Phys.*, **87**, 5968 (1987).
40. (a) R. Krishnan, J. S. Binkley, R. Seeger, and J. A. Pople, *J. Chem. Phys.*, **72**, 650 (1980); (b) T. Clark, J. Chandrasekhar, G. W. Spitznagel, and P. R. von Schleyer, *J. Comput. Chem.*, **4**, 294 (1983).
41. J. L. Pascual-Ahuir, E. Silla, and I. Tunon, *J. Comput. Chem.*, **15**, 1127 (1994).
42. M. Cossi, B. Menucci, and R. Cammi, *J. Comput. Chem.*, **17**, 57 (1996).
43. F. Floris, J. Tomasi, and J. L. Pascual-Ahuir, *J. Comput. Chem.*, **12**, 784 (1991).
44. R. Pierotti, *Chem. Rev.*, **76**, 717 (1976).
45. J. Pranata and G. D. Davis, *J. Phys. Chem.*, **99**, 14340 (1995).
46. R. D. Brown, P. D. Godfrey, and B. J. Kleibomer, *J. Mol. Struct.*, **124**, 34 (1987).
47. J. Floriàn and B. G. Johnson, *J. Phys. Chem.*, **99**, 3681 (1994).
48. V. Barone and C. Adamo, manuscript in preparation.
49. V. Barone and R. Arnaud, *J. Chem. Phys.*, **106**, 8727 (1997).